

A COMPREHENSIVE HIDDEN MARKOV MODEL FOR HOURLY RAINFALL TIME SERIES

BY OLIVER STONER* AND THEO ECONOMOU

Department of Mathematics, University of Exeter

For hydrological applications, such as urban flood modelling, it is often important to be able to simulate sub-daily rainfall time series from stochastic models. However, the literature is currently lacking owing to several challenges with modelling rainfall at this resolution, namely a complex temporal structure including long dry periods, seasonal variation in both the occurrence, and intensity of rainfall, and extreme values. To address this, we propose a flexible model, an advanced hidden Markov model set in the Bayesian hierarchical framework, which is capable of capturing and reproducing these characteristics well. To demonstrate this, we apply the model to an 8-year time series of hourly observations. We also present thorough model checking and a critical discussion of our approach.

1. Introduction. Severe flooding events, such as those that occurred in the UK in the winter of 2013-2014 and the winter of 2015-2016, pose a great risk to society. For each winter, the total economic damage caused by the flooding was estimated to be over one billion pounds (GBP) of economic damage ([Environment Agency \(2016\)](#), [Environment Agency \(2018\)](#)). Hydrological flood models play an important role in mitigating this damage, including by helping to inform the planning of new flood defences and drainage systems, as well as integration with flooding warning systems.

Typically, hydrological models are used to test the response of the hydrological system to design storms, which are intended to represent an idealised extreme rainfall scenario. However, [Chandler et al. \(2014\)](#) argue that this approach is limited, in the first instance because the temporal profile of the design storm may fail to capture important characteristics of system performance. Moreover, focusing on the response of the system to a single event may be inadequate, as the risk of flooding posed by a single storm event depends strongly on the antecedent conditions of the catchment ([Chandler et al., 2014](#)). For example, the risk of flooding may depend on whether or not the catchment has already been saturated by recent rainfall. For this rea-

*Oliver Stoner was supported by a NERC GW4+ Doctoral Training Partnership studentship from the Natural Environment Research Council [NE/L002434/1].

Keywords and phrases: Extreme values, Bayesian methods, non-homogeneous, generalized Pareto distribution, zero-inflation, splines.

son, [Chandler et al. \(2014\)](#) argue that hydrological models should instead use long rainfall time series generated from stochastic/probabilistic models as inputs, so that the effects of both the rainfall intensity during a storm event and antecedent conditions can be taken into account.

Modelling rainfall is challenging because its natural variability can dominate any seasonal structures or long-term temporal trends, more so than other meteorological variables such as temperature and wind ([Chandler et al., 2014](#)). For this reason, it is vitally important to capture well the whole distribution of rainfall values, which is in itself a non-trivial task due to the propensity of extremely high rainfall values. This is illustrated in the left plot of Figure 1, which shows empirical quantiles of non-zero rainfall gauge observations from an 8-year hourly time series in Exeter, UK. The heavy tail is especially clear when comparing the highest hourly values (well over 20mm) to the 99% quantile, which is only 5.2mm. Ensuring the model is capable of reproducing these extremes is essential in any application where they are of great concern, such as surface flood modelling. An equivalent return-level plot can be found in the supplementary material.

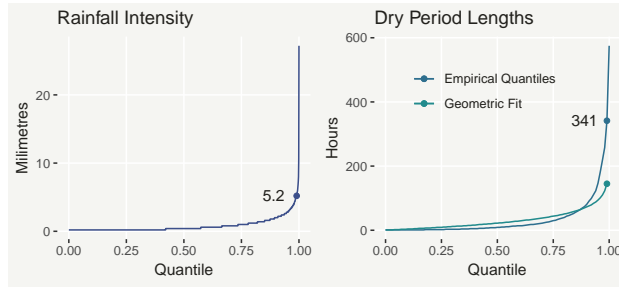


FIG 1. *Empirical quantiles of the hourly rainfall intensities (observations greater than 0mm) from the Exeter gauge time series (left), empirical quantiles of dry period lengths (where rainfall does not exceed 0.2mm in any given hour), and theoretical quantiles of a Geometric fit. The points are 99% quantiles.*

A further modelling challenge is the complex temporal structure in the occurrence of rainfall, which notably consists of long dry periods. To illustrate this, the right plot in Figure 1 shows the empirical quantiles of dry period lengths (defined as periods where the hourly rainfall value does not exceed 0.2mm). This distribution also has quite a heavy tail, including several high values which may be considered extremes. Capturing these extremes is equally important, particularly for applications where droughts are a concern, such as agricultural planning.

Finally, both rainfall intensity and occurrence can vary substantially by season. In the UK for instance, summer rainfall extremes tend to be more severe than in the winter ([Chandler et al., 2014](#)). For this reason, care should be taken to ensure model simulations accurately reflect the time of year.

In this article we argue that there is currently a lack of a sub-daily rainfall

model which is capable of capturing key features of rainfall well, notably:

- Seasonal and temporal variation in occurrence and intensity;
- Long dry periods (which vary with time and season);
- Extreme values (which vary with time and season).

To address this, we propose a comprehensive model for hourly rainfall gauge data, based on an advanced hidden Markov model (HMM). Given that such stochastic rainfall models are often used in decision making (e.g. warnings) or as inputs to physical models (e.g. hydrological), a further requirement is that uncertainty is fully quantified and propagated in the output. As such the proposed models are implemented in the Bayesian hierarchical framework. Applied to 8 years of hourly rainfall gauge data, we demonstrate using posterior predictive model checking how our proposed model performs well overall and specifically with respect to capturing these three features.

The article is structured as follows: Section 2 gives an overview of existing approaches to stochastic/statistical modelling of rainfall, highlighting their strengths and limitations. In Section 3, we propose a flexible model for sub-daily rainfall gauge time series, which we then apply to an 8-year long time series of hourly observations. In Section 4, we present extensive model checking and an analysis of model output. Finally, the article ends with a critical discussion of our approach in Section 5.

2. Background. In the previous section we outlined features of rainfall occurrence and intensity, namely long dry periods and extremely high values, which make modelling challenging. Aggregating rainfall observations into a coarser temporal resolution, such as daily values, can help to smooth-out these features and make modelling more straightforward. [Chandler et al. \(2014\)](#) present a thorough review of the vast daily rainfall modelling literature, discussing various modelling approaches which have addressed these challenges. Some notable approaches to modelling daily rainfall include those based on the Generalized Linear Model (GLM) framework (e.g. [Yang et al. \(2005\)](#)), those based on hidden Markov models (e.g. [Kim and Lee \(2017\)](#)) and those based on latent spatio-temporal fields (e.g. [Kleiber et al. \(2012\)](#)).

However, [Segond et al. \(2007\)](#) argue that, while daily rainfall time series may be suitable as inputs of flood modelling in rural catchments, for urban catchments a higher temporal resolution is necessary, as the response of the system may develop on a shorter time-scale.

2.1. Indirect rainfall models. All of the aforementioned approaches can be characterised as attempts to directly model the observed rainfall at a given time as arising from some probabilistic model. However, owing to the

increased complexity of the temporal structure of sub-daily rainfall, these approaches may not always work well.

An alternative approach to modelling rainfall is to instead stochastically model the larger structures which generate rainfall, such as storm events. Given the occurrence of such structures, the amount of rainfall over a time period is then deterministic, based on some simplifying assumptions (see for instance [Rodriguez-Iturbe et al. \(1987\)](#)). Several parameters control different aspects of the model, such as storm event duration, frequency of occurrence, and intensity. Through these parameters, it is possible to tune the model to capture certain properties of the observed data, such as the length of dry periods, temporal dependence and the distribution of non-zero rainfall.

Whilst these approaches consist of few parameters and are in some sense based on physical justification, the absence of a likelihood function on which to base inference makes implementation challenging. This means it is often necessary to rely on alternative methods of implementation, such as by maximising objective functions (potentially missing out on parametric uncertainty) or by employing Approximate Bayesian Computation (ABC), which requires the careful selection of summary statistics ([Aryal and Jones, 2017](#)). Furthermore, it is not evident that these approaches are able to reproduce extreme rainfall values well, a feature which [Chandler et al. \(2014\)](#) argue is lacking in the sub-daily rainfall modelling literature. For these reasons, we pursue a fully probabilistic framework to directly model the distribution of rainfall in time. We argue that direct characterisation of the distribution constitutes a more interpretable framework, particularly in terms of model expansion and checking.

2.2. Hidden Markov models (HMMs). One family of probabilistic models that has been used extensively for rainfall data (e.g. [Kim and Lee \(2017\)](#), [Rayner et al. \(2016\)](#)), to capture temporal structures in both rainfall occurrence and intensity, is hidden Markov models (HMMs). In HMMs, a hidden, unobservable quantity z_t varies over discrete time steps, alternating between a finite number Z of values or states $z_t \in \{S_1, \dots, S_Z\}$. Variable z_t is a discrete Markov chain, whose evolution over time is probabilistic, governed by a transition matrix P of probabilities. The particular state the hidden variable is in at a given time step affects (the parameters of) the conditional model for the observed quantity, which in the case of rainfall translates to the model(s) for occurrence and intensity. HMMs are useful for rainfall because they can capture its temporal behaviour through the Markovian structure of the latent chain, without the need to explicitly include climatological structures, such as the arrival of weather fronts, or other physical processes.

Conventional HMMs for rainfall often suffer from a number of shortcomings, such as underestimation of the length of long dry periods (Chandler et al., 2014). However, their flexibility as a framework, afforded by the freedom to specify virtually any conditional model for occurrence and intensity, means that it may be possible to address these issues through a number of extensions. Based on this idea, in the subsequent section we will present our approach to modelling rainfall gauge data, which we argue is capable of capturing all the key features of rainfall data identified in Section 1.

3. Methodology.

3.1. *Conventional HMMs for rainfall.* It is instructive to begin by defining a basic and generic HMM for rainfall. Capturing the whole distribution (tails and bulk) of rainfall well is challenging, but one way of doing so is through a discrete mixture of, say $Z = 3$, distributions. These can be interpreted as rainfall severity states, i.e. “dry”, “wet”, “wetter”. A discrete random quantity $z_t \in \{1, 2, 3\}$ is used to characterize the distribution of rainfall y_t as:

$$(1) \quad f(y_t) = \sum_{j=1}^Z \mathbb{1}(z_t = j) f(y_t | z_t)$$

where $\mathbb{1}$ is the identity function, and $p(y_t | z_t)$ is the conditional distribution of rainfall y_t for each state. HMMs allow for temporal dependence by assuming that z_t is an unobserved discrete Markov chain, so that temporal structure is introduced in the persistence of each state. This is parametrised by a transition matrix $P = \{p_{i,j}\}$ where $p_{i,j} = \Pr(z_t = j | z_{t-1} = i)$.

Such models are conventionally homogeneous, meaning that the transition between states in the HMM is time invariant. However, this does not allow for the effect of seasonal variation or climatological covariates on the temporal structure of rainfall. Several articles (such as Spezia (2006), Meligkotsidou and Dellaportas (2011), Antonello and Roberto (2012)) have instead presented non-homogeneous hidden Markov models (NHMMs), where covariates are used to characterise the parameters of the transition matrix. This added flexibility could be used to allow for seasonal or long term heterogeneity in the temporal structure of rainfall.

Additionally, HMMs are limited by the fact that the number of time steps the hidden variable z_t persists in a given state is implicitly Geometrically distributed. The right plot of Figure 1 illustrates that Exeter’s dry period length distribution has a very heavy tail, with several dry periods lasting hundreds of hours. This would be a concern if the HMM consists of only

one dry state and hence relies on an implicit geometric model to capture this distribution, which we illustrate by also plotting a method of moments Geometric fit to the dry period lengths.

Including additional unique ‘dry states’, which the hidden state parameter could transition between, may introduce sufficient flexibility to capture the longest dry periods. However, this would impede the physical interpretability of the model and potentially introduce identifiability issues. If it is the case that the dry period distribution is seasonally structured, then some improvement may be possible by introducing non-homogeneity to the dry state, though this may still be insufficient.

A more potent solution would instead be to use a hidden semi-Markov model (HSMM), where the persistence distribution is explicitly defined and thus can be chosen to have a heavier tail. However, HSMMs are often impractical and too computationally expensive to implement. This is especially true when the total number of time steps T is large, as many of the implementation methods have an algorithmic order $O(Z^2T^2)$ or even $O(Z^2T^3)$, compared to only order $O(Z^2T)$ for HMMs. Often, it is necessary to restrict the upper bound of the support of the persistence time distribution prior to fitting the model, to ensure computational feasibility (Economou et al., 2014). However, this strong prior statement about the persistence distribution can lead to invalid parameter estimates (Dewar et al., 2012). While this issue can be overcome by making the restriction adaptive in the implementation process, the method is still of far greater computational complexity than the basic HMM.

Once an appropriate choice of temporal structure is made, it remains to specify the conditional rainfall model. This usually involves the mixture of a Bernoulli quantity, which represents the occurrence of rainfall, and a strictly positive quantity, to represent the intensity of rainfall, conditional on occurrence. The choice of distribution for the positive rainfall values is made more difficult by the presence of extremely high observations. For many applications of a statistical rainfall model, including urban flood modelling, the risk posed by these extreme events are of particular concern. Furrer and Katz (2008) argue that the commonly used Gamma distribution is not able to capture these extremes well. While some authors prefer to use the Weibull distribution (Bruno et al., 2008), Furrer and Katz (2008) also concluded that this distribution is lacking.

Several approaches, such as Li et al. (2012) aim to better capture extremes by mixing a more typical distribution, in this case the Exponential distribution, with the Generalised Pareto distribution for values above a given threshold, which is estimated by imposing a continuity constraint on the

two distributions. However, [Furrer and Katz \(2008\)](#) also found that these approaches, while still performing better than the Gamma and Weibull distributions, are not able to capture well the likelihood of extreme values.

In what follows, we present an extended HMM-based framework that is flexible enough to adequately capture both temporal persistence and extremes in rainfall, while retaining interpretability.

3.2. An extended rainfall HMM. We begin by considering the basic three-state HMM introduced earlier. One state is intended to capture dry periods, while the remaining two are intended to capture wet periods. These wet states may end up representing periods of low and high rainfall intensity, respectively, or may differ in how long they last or how often they occur.

The HMM structure for z_t is defined by an initial state probability vector P_0 and a transition matrix:

$$(2) \quad P = \begin{pmatrix} p & q_1(1-p) & q_2(1-p) \\ r_{1,1} & r_{1,2} & r_{1,3} \\ r_{2,1} & r_{2,2} & r_{2,3} \end{pmatrix}$$

For reasons that will soon be clear, we parametrise the first row (corresponding to the dry state) in terms of the probability of remaining in the dry state (p), and the conditional (on a transition out of the dry state) probabilities of transitioning into each wet state, q_1 and q_2 such that $q_1 + q_2 = 1$. As discussed in [Section 2](#), a restriction of this model is that the length of time spent in the dry state has an implicit Geometric(p) distribution, which may not be sufficiently flexible to capture long dry periods. For a long time series, such as $t = 1, \dots, 70128$ hours in our application later on, an HSMM framework is prohibitively computationally expensive, so here we look for ways to retain the practicality of HMMs while making them more flexible in terms of capturing long persistence periods.

[Zucchini et al. \(2017\)](#) present a way of achieving a more flexible persistence distribution for a given state, without losing the convenience the HMM framework. For clarity of exposition, denote the dry state as d and the wet states as w_j for $j = 1, 2$. The idea is to introduce a number of “clone” dry states d_1, \dots, d_D , which are all identical to each other and to the original dry state d , in the sense that they all have the same conditional model. The transition matrix is then defined in such a way that transitions from w_j are only possible to the first clone state d_1 . From here, the hidden chain can persist in the first clone state d_1 with probability p_1 , or transition to w_j , or transition to the second clone state d_2 . If the chain transitions to d_2 , it can remain there with probability p_2 , or transition to d_j or to the next clone

state d_3 , and so on. The motivation behind this approach is that, while the number of time steps spent in each of the clone states is still Geometric, the total amount of time spent in any of the clone states before transitioning to another unique state w_j is a more flexible distribution – essentially a weighted sum of Geometric distributions. Note that the dry state d is now only implicitly defined in the sense that all clone states relate to the same conditional model for “dryness” (low rainfall).

We also employ an approach that is based on the introduction of clone states. However, our formulation is such that it allows for modelling flexibility, particularly in terms of introducing temporal non-stationarity in the persistence of the dry state. To that end we consider the following constrained transition matrix:

$$(3) \quad P = \begin{pmatrix} p_1 & \cdot & 0 & q_1(1-p_1) & q_2(1-p_1) \\ \cdot & \cdot & \cdot & \cdot & \cdot \\ 0 & \cdot & p_D & q_1(1-p_D) & q_2(1-p_D) \\ v_1 r_{1,1} & \cdot & v_D r_{1,1} & r_{1,2} & r_{1,3} \\ v_1 r_{2,1} & \cdot & v_D r_{2,1} & r_{2,2} & r_{2,3} \end{pmatrix}$$

Here, transitions are possible from wet states w_j into any of the clone dry states d_i , while no transitions between the clone states are possible. The latter is achieved by constraining the off-diagonal entries of the first D rows and columns to be zero. The result of this is that, while the dry state persistence distributions are each Geometric(p), p can now be thought of as a (categorical) random quantity taking values in $\{p_1, p_2, p_3\}$, such that the marginal distribution for the time spent in the implicit dry state is, like the approach in [Zucchini et al. \(2017\)](#), a more flexible Geometric mixture.

To ensure that it is possible to conceptualise the clone dry states as a single state, further constraints are imposed on the transition matrix: First, conditional on a transition from a dry state to a wet state, the transition probabilities (q_1 and q_2) into each wet state are invariant of the dry state. Second, conditional on a transition from a wet state to a dry state, the transition probabilities (p_1, \dots, p_D) into each dry state are invariant of the wet state. These are in addition to the constraint that the conditional model for rainfall occurrence and intensity is the same for all of the dry states.

This approach is equivalently flexible to the one presented in [Zucchini et al. \(2017\)](#), in the sense that it is capable of better capturing heavy tailed persistence distributions. This implies that, without sacrificing the physical interpretability of having only one dry state, or the practicality of the HMM framework, extra flexibility has been afforded to potentially capture better the longest dry periods. However, as the parameters of the transition

matrix are constant in time, the model can't capture seasonal or annual variation in the expected length of dry periods which may be, for example, longer on average in the summer than in the winter. The advantage of our approach is that it is straightforward to directly model the dry state persistence probabilities p_1, \dots, p_D as temporally-varying. One way of achieving this, as defined in (4), is a logistic model for the dry state persistence probabilities. Here $u(t, d)$ represents a general model of time $t = 1, \dots, T$ and hidden state $d = 1, \dots, D$, which may also include covariate effects such as large scale climate indices such as the North Atlantic Oscillation (NAO).

$$(4) \quad \log \left(\frac{p_d(t)}{1 - p_d(t)} \right) = u(t, d)$$

For our application to the Exeter data, we characterise $u(t, d)$ by combining an intercept term $\iota(d)$ which is different for each clone dry state, and two penalised splines which are common across the states:

$$(5) \quad u(t, d) = \iota(d) + a_1(t) + a_2(t).$$

The first spline, $a_1(t)$, is a cyclic (the two end points have equal value) cubic spline of the time of year, which is intended to capture seasonal variation in the length of dry periods. The second, $a_2(t)$, is a cubic spline of time overall, which is intended to capture between-year variation in the average length of dry periods. The use of splines affords the model flexibility to capture different dry period persistence structures which may occur in different climatic conditions, and also to better capture very long dry periods.

3.3. Conditional rainfall model. Having specified a non-stationary (non-homogeneous) and essentially semi-Markovian latent structure, it remains to define a conditional model for rainfall occurrence and intensity. First recall the notation $z(t)$, the latent state at any given time point. Continuing with our three state example, $z(t)$ takes only 3 values (dry, wet, wetter), noting that the dry state is made up of D clone dry states, among which the conditional model is the same.

As zero rainfall is generally a common observation (approximately 88% of all observations in the Exeter time series), it makes sense to mix a continuous distribution for rainfall intensity with a probability mass at zero. This probability of zero rainfall, π_t , should vary with the latent state z_t , for example it should be higher in the dry state than in the wet states, and it may also vary with time and/or depend on climatological covariates. We achieve this by employing a logistic model for π_t :

$$(6) \quad \log \left(\frac{\pi_t}{1 - \pi_t} \right) = v(t, z_t)$$

For our application to the Exeter gauge, we once again employ a combination of a season and an overall temporal spline:

$$(7) \quad v(t, z_t) = \eta(z_t) + b_1(t, z_t) + b_2(t, z_t)$$

Unlike the splines for the dry state persistence probabilities, splines $b_1(t, z_t)$ and $b_2(t, z_t)$ are different and independent across each of the three states.

As discussed in Section 3.1, there are many choices for the distribution of rainfall intensity, including Gamma, Weibull, Log-Normal and hybrid distributions. One of the key advantages of the approach we advocate is that it is possible to choose from any of these or any other distributions, even using different distributions for each state if desired. Recalling that one of our key modelling aims is to capture extreme values well, for the Exeter data we opt for the zero-location (zero-threshold) Generalized Pareto distribution (GPD), with scale parameter σ_t and shape parameter ξ_t :

$$(8) \quad \log(\sigma_t) = \alpha(z_t) + c_1(t, z_t) + c_2(t, z_t),$$

$$(9) \quad \xi_t = \gamma(z_t) + d_1(t, z_t) + d_2(t, z_t).$$

Once more we make use of seasonal ($c_1(t, z_t)$ and $d_1(t, z_t)$) and temporal ($c_2(t, z_t)$ and $d_2(t, z_t)$) splines to capture inhomogeneity. By including independent splines for each state in all of the parameters of the conditional model (in this case π_t , σ_t and ξ_t), a high degree of flexibility for capturing seasonal and temporal variation in the rainfall distribution is afforded.

In our dataset, the hourly observations are rounded to the nearest 0.2mm, which means that the likelihood should be adjusted accordingly. For example, if a rainfall observation is 2mm, the contribution to the likelihood should not just be the density $f(2mm; \dots)$, but should instead be $P(1.9mm < X \leq 2.1mm)$. Furthermore, we truncate the GPD at 0.1mm such that the zero probability accounts for all values less than 0.1mm (which would be rounded to zero), such that the complete density function is:

$$(10) \quad f(x; \pi, \sigma, \xi) = \begin{cases} \pi & x = 0 \\ (1 - \pi) \frac{F(x+0.1) - F(x-0.1)}{1 - F(0.1)} & x = 0.2, 0.4, \dots \end{cases}$$

where F is the cumulative distribution function of the zero-location GPD:

$$(11) \quad F(x; \sigma, \xi) = 1 - \left(1 + \frac{\xi x}{\sigma}\right)^{-\frac{1}{\xi}}$$

3.4. *Prior distributions and implementation.* We apply the model to hourly observations from the Exeter International Airport rainfall gauge, a time series of 70128 values spanning the 8-year period 2010 to 2017.

To keep the model as general as possible, we specified uniform Dirichlet(**1**) prior distributions for transition matrix parameters \mathbf{v} , \mathbf{r}_1 and \mathbf{r}_2 . We also specified non-informative Normal($0, 10^2$) prior distributions for the intercept parameters $\iota(d)$, $\eta(z_t)$, $\alpha(z_t)$ and $\gamma(z_t)$, where we use $d = 1, 2, 3$ clone dry states. However, a common problem with hidden Markov models is label switching, where the conditional models of one or more states swap. When this happens, the overall model is the same but parameter inference is convoluted, especially in a Bayesian implementation where Markov Chain Monte Carlo (MCMC) is employed. To prevent this, we impose the following constraints on the intercept parameters:

$$(12) \quad \iota(1) > \iota(2) > \iota(3)$$

$$(13) \quad \eta(1) > \max(\eta(2), \eta(3))$$

$$(14) \quad \gamma(3) > \gamma(2)$$

Constraints (12) and (13) do not really restrict the model, they just order the clone dry states and specify that the dry states should have a higher average probability of zero rainfall than the two wet states, respectively. The third constraint (14), that the second wet state should have a heavier tail behaviour on average, regardless of the scale parameter, can be viewed as a potential restriction, but this can justified subject to satisfactory model checking performance.

All splines were set up using the `jagam` function in the `mgcv` package for the programming language R (R Core Team, 2019). We specified 6 equidistant knots for the seasonal splines and 1 knot for each year (8 in total) for the overall temporal splines. For each spline, the coefficients are assigned Multivariate-Normal priors (Wood, 2016) where the covariance matrix is scaled by parameter ν (unique for each spline), which acts as a smoothing penalty where smaller values of ν correspond to a stricter penalty. More generally, this penalty is intended to avoid over-fitting, but for this application we would like our spline effects to be quite smooth as they are only intended to capture long-term variation, while the HMM latent state z_t is intended captures short to medium term variation. For these penalty parameters (ν), we specified Half-Normal($0, \sqrt{2}^2$) prior distributions, which corresponds to a modest smoothness penalty.

The model was implemented using the `nimble` package (de Valpine et al., 2017), a comprehensive suite for highly flexible MCMC inference. In this

case, we needed to create a custom likelihood function for the rainfall observations which incorporates a version of the recursive forward algorithm used to compute the marginal likelihood in HMMs (Scott, 2002) and thus avoiding sampling the latent states. This was adapted to allow for a temporally-varying transition matrix. We ran four MCMC chains for a total of 20k iterations, discarding the first 10k as burn-in. Owing to the complexity and size of the model (70128 hours of data), the model takes 2-3 days (on an Intel Core i9-7900X processor with 64GB of memory) with the four chains running in parallel. Each chain was randomly initialised at different parameter values and was assigned a different random number generator seed. Convergence of the four chains was assessed by visual inspection of trace plots and by computing the Potential Scale Reduction Factor (MPSRF) (Brooks and Gelman, 1998) for all of the following parameters: the initial state probability P_0 ; static transition matrix parameters (\mathbf{q} , \mathbf{v} and \mathbf{r}), all of the intercepts ($\boldsymbol{\iota}$, $\boldsymbol{\eta}$, $\boldsymbol{\alpha}$ and $\boldsymbol{\gamma}$); and all of the spline coefficients. This metric compares the variance between the chains to the variance within the chains. If the two variances are similar for a given parameter then this typically results in an PSRF of less than 1.05. Starting from different initial values and obtaining an PSRF of less than 1.05 gives the best indication that the chains have converged to the posterior distribution. Figure 2 shows a histogram of computed PSRFs. For the overwhelming majority of parameters, the PSRF is small (less than 1.05), suggesting the chains have converged.

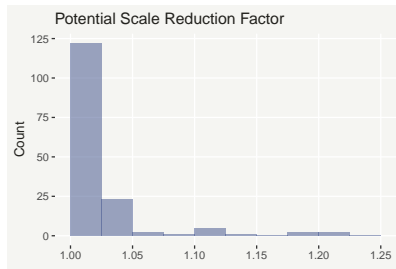


FIG 2. Histogram of computed potential scale reduction factors.

4. Model Checking and Results. In this section we illustrate the model’s performance through comprehensive model checking and analysing some key results. We do the former by simulating a new time series of length 70128, $\tilde{\mathbf{r}}$, from each posterior sample. Doing this, we have 4000 simulated time series (after thinning the posterior samples by 10) and the general principle is then to assess whether certain characteristics of the observed values \mathbf{r} are extreme relative to simulations from the model (Gelman et al., 2014).

4.1. *Temporal structure.* We begin by assessing the model’s ability to capture long dry periods, one of the three key characteristics of rainfall data we identified as important in Section 1. We do this by, for each simulated time series \tilde{r} , calculating the length of all dry periods (defined as periods where rainfall does not exceed 0.2mm in any hour), sorting them into ascending order and storing the 800 greatest lengths (as there is a different number of dry periods in each simulated time series). Figure 3 shows the median predicted 800 greatest dry period lengths, with 95% prediction intervals, compared to the 800 greatest dry period lengths in the observed data. The model generally does an excellent job of capturing the distribution of dry period lengths, with the median values tracking the observed values (diagonal line) very closely, all the way up until the last few points, which are still contained within the 95% prediction intervals. In developing our approach, we found that the inclusion of ‘clone’ dry states made a dramatic improvement over the baseline HMM in capturing this distribution well (the baseline was not able to capture any part of this distribution remotely well), but it wasn’t quite good enough until we allowed the dry persistence probabilities to vary with time.

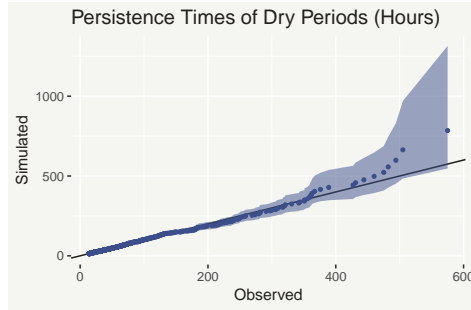


FIG 3. Median simulated 800 longest sorted dry periods, defined as periods where rainfall does not exceed 0.2mm in any one hour, compared to the 800 longest observed periods and with associated 95% prediction intervals.

We move on to assessing the temporal structure more generally, which we do by calculating the Spearman auto-correlation, at various lags, for each simulated time series \tilde{r} . Here, the lag-1 autocorrelation means the correlation between rainfall values one hour apart (the correlation between the two vectors $\tilde{r}_1, \dots, \tilde{r}_{70127}$ and $\tilde{r}_2, \dots, \tilde{r}_{70128}$), lag-2 is the correlation between values two hours apart and so on. We can then compare the corresponding autocorrelations for the observed data to the distribution of simulated autocorrelations. Figure 4 shows the density estimates of simulated lag-1, lag-2, lag-6 and lag-24 autocorrelations. None of the observed autocorrelations are extreme with respect to the distributions of simulated statistics, hence this check suggests the model is generally capturing the temporal structure well.

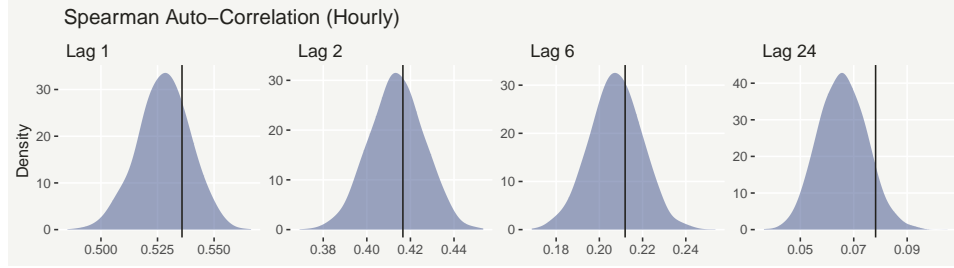


FIG 4. *Density plots of simulated Spearman autocorrelations from the model, with vertical lines representing the corresponding observed autocorrelations.*

4.2. Seasonal distributions. Whilst capturing the whole distribution of hourly rainfall values well, including extremes, can be challenging in itself, an even greater challenge is capturing this distribution as it varies by season. For example, many models overestimate extremes in the winter and underestimate them in the summer (Chandler et al., 2014).

First we check that the model is able to capture seasonal variation in the occurrence in rainfall. Figure 5 shows density plots of the proportion of zero values in each calendar season from the simulated time series $\tilde{\mathbf{r}}$, compared to the proportions in the observed values. All of the observed values are captured quite well, for example the model captures the increased proportion of zeros in the summer compared to the winter, so it's clear that the model is able to reproduce seasonal variation in rainfall occurrence.

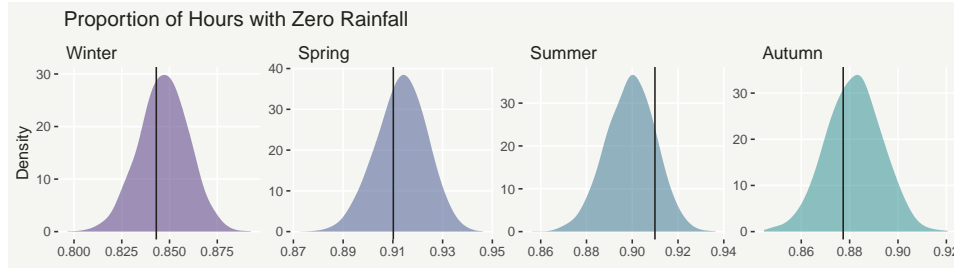


FIG 5. *Median predicted sorted rainfall values, from 4000 simulated 8-year time series, with associated 95% credible intervals.*

Next we check whether the model is able to capture seasonal variation in rainfall intensity. We do this for each season, by sorting (ranking) each simulated rainfall time series $\tilde{\mathbf{r}}$, and then compare the distribution of intensities for each rank to the observed ranked intensity (this has a similar interpretation to a quantile-quantile plot). Figure 6 compares the observed

sorted values to the median simulated sorted values, with associated 95% prediction intervals. Looking at the plots, it's clear that the distribution of rainfall values varies greatly by season, with higher (and more extreme) rainfall values in the summer and the autumn than in the winter and the spring. Despite this variation, the model is able to capture each season's distribution very well, all the way up to the extremes, especially given only two wet states were used.

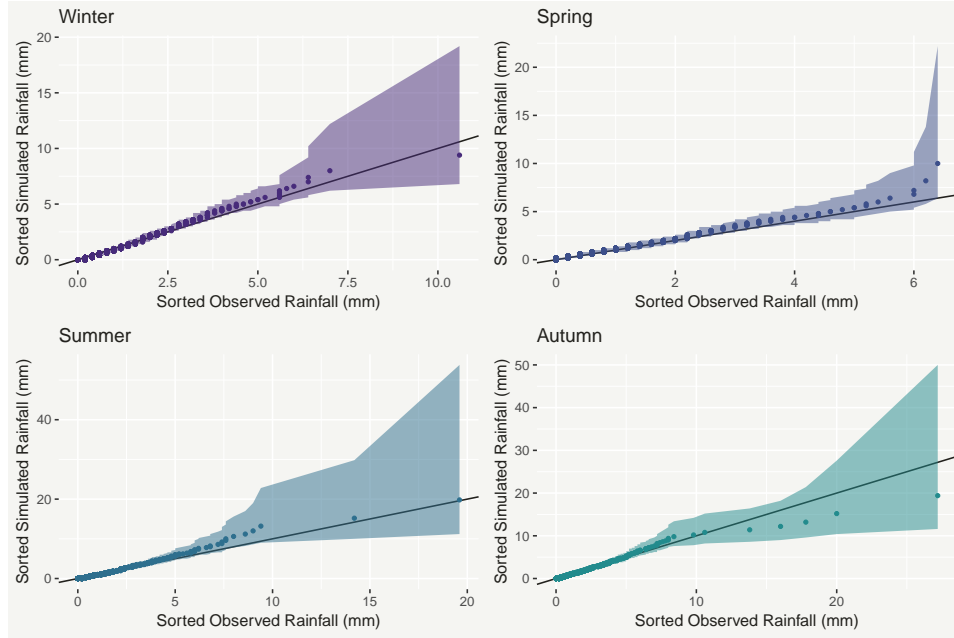


FIG 6. Median predicted sorted rainfall values, from 4000 simulated 8-year time series, by calendar season and with associated 95% prediction intervals.

4.3. Daily and monthly rainfall checking. For some applications it may also be important that the model captures well the cumulative rainfall over a longer time period, such as a day, or a month. To assess this, we aggregate both the observed time series \mathbf{r} and each simulated time series $\tilde{\mathbf{r}}$ (as detailed in Section 4) into daily values and monthly values. We can now assess whether the aggregated data ($\mathbf{r}_{\text{daily}}$ and $\mathbf{r}_{\text{monthly}}$) is extreme with respect to the simulated data ($\tilde{\mathbf{r}}_{\text{daily}}$ and $\tilde{\mathbf{r}}_{\text{monthly}}$).

First we check that the model captures the distribution of daily rainfall intensity well. Figure 7 shows predicted sorted values from the model, compared to the sorted observed values. The model captures most of the distribution excellently, though there is some deviation in the very upper

tail. In this region, the observed values are either contained by or extremely close to the 95% prediction intervals, and the highest values are actually captured very well, so we believe the model is doing well enough.

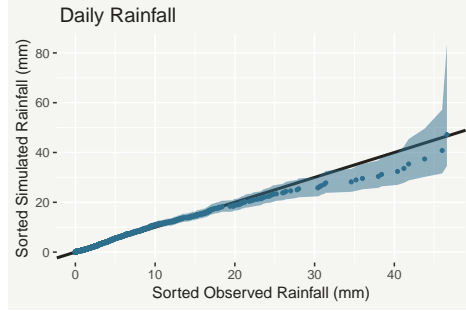


FIG 7. Median sorted simulated daily rainfall values, with 95% prediction intervals, compared to the corresponding sorted observed values.

Similarly, we can also check the model captures the distribution of monthly rainfall intensity well. Once again, the model captures most of the distribution virtually perfectly, with some mild deviation in the very upper tail but not to a concerning extent.

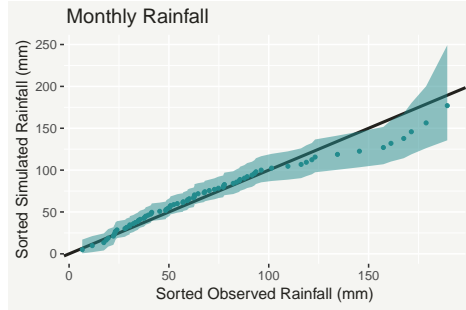


FIG 8. Median sorted simulated monthly rainfall values, with 95% prediction intervals, compared to the corresponding sorted observed values.

4.4. *Temporal effects.* As well as aiding in fitting the data better, the temporal effects can indicate how different characteristics of rainfall vary with time of year and between years. Figure 9 shows the posterior median predicted effects of time of year (left) and time overall (right) on the expected persistence of dry periods, as defined by (5). Looking at the cyclic effect of time of year, there is overwhelming evidence that dry periods are longer in the warmer months (May-September) than the rest of the year. Looking at the overall temporal effect, there isn't very strong evidence of any change in the expected length of dry periods over the 8 years.

Figure 10 shows the effects of time of year (left column) and overall time (right column) on the conditional probability of zero rainfall (top row) and the distribution of rainfall intensity, through the Generalized Pareto scale

and shape parameters (central and bottom rows, respectively). First note that the zero probability spline for wet state 2 isn't plotted, because the zero probability in wet state 2 was so low that the spline had no predicted effect and was very uncertain. Similarly, the dry state converged to a situation where it essentially produced exclusively values of 0mm and 0.2mm, meaning the splines for the scale and shape parameters also had no predicted effect.

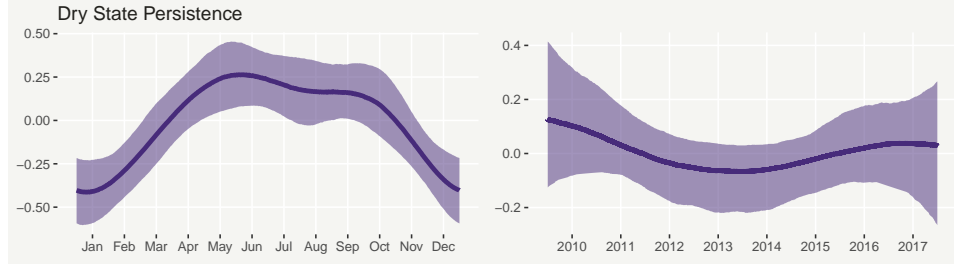


FIG 9. *Posterior median predicted effect of the time of year (left) and overall time (right) on the dry state persistence probabilities, with 95% credible intervals.*

Looking at the cyclic effects, there is a clear pattern where the conditional probability of zero rainfall is higher in the warmer months in both the dry state and wet state 1. This is in addition to the longer dry periods seen at this time of year in Figure 9. Now looking at the effects for wet state 2, we can see that both the shape and scale are higher in the summer and autumn than elsewhere in the year, meaning both higher average rainfall values and a heavier tail behaviour. Interestingly, the scale parameter is at its highest in the autumn, while the shape parameter is highest in the summer. This makes sense to us because our anecdotal experience of Exeter is that autumn is more consistently rainy, while summer is prone to intermittent downpours. The seasonal intensity effects for wet state 1 don't show a similarly strong pattern, indicated by the 95% credible intervals containing zero.

The overall temporal effects show several strong (in terms of 95% credible interval certain) trends over the 8-year time series. For example, the scale parameter of wet state 2 is highest around 2013, which may correspond to the occurrence of severe storm events around this time (e.g. [Environment Agency \(2016\)](#)). These effects seem to be capturing real trends, rather than just sampling variation between the years, though a substantially longer time series may be necessary to investigate whether they relate to large scale climate indices like the NAO.

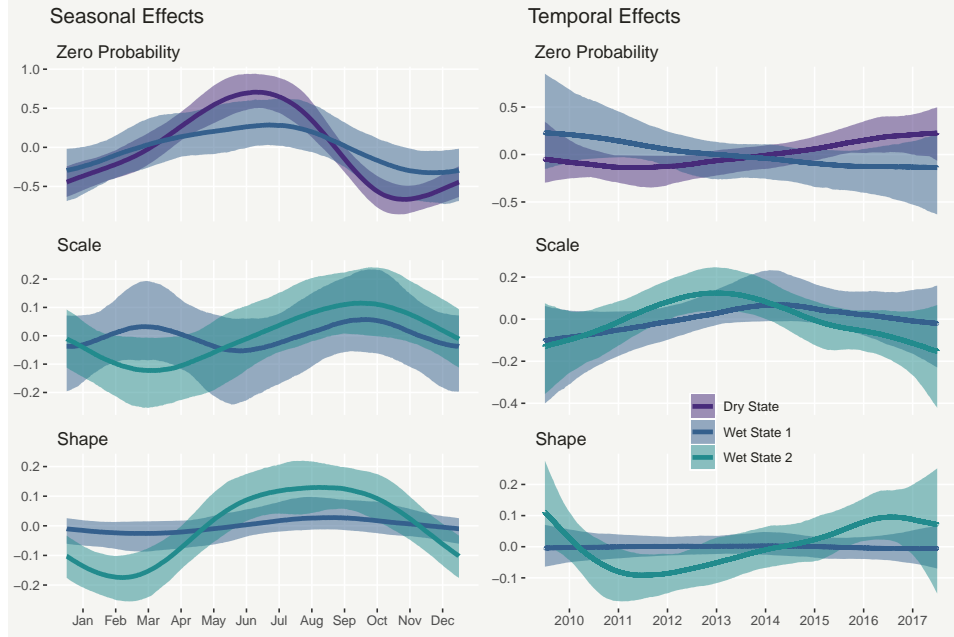


FIG 10. *Posterior median predicted effects of time of year (left column) and overall time (right column) on the conditional probability of zero rainfall (top row), and the Generalized Pareto scale and shape parameters (central and bottom rows, respectively), by hidden Markov state and with 95% credible intervals.*

5. Discussion. In this article we discussed the role of stochastic or statistical rainfall modelling in the context of hydrological applications, such as urban flood modelling. We identified a lack of a comprehensive model for sub-daily rainfall which is able to capture all of the following crucial features: seasonal variation in rainfall occurrence and intensity, long dry periods and extreme values. To address this, we presented a flexible model, based on a hidden Markov model and set in the Bayesian hierarchical framework, which makes several innovations compared to conventional approaches. These included clone states and temporal non-homogeneity in the transition matrix, which together allow the model to capture even the longest dry periods.

To demonstrate the effectiveness of our approach, we applied a relatively simple model comprising 3 cloned dry states and 2 wet states to an 8-year long time series of hourly values from a rainfall gauge in Exeter, UK. We found that the model is able to capture well the distribution of dry period lengths, seasonal variation in occurrence and intensity (including extreme values) and the distribution of intensity when aggregated to daily and monthly resolutions. We also illustrated how the model output can be

interpreted in terms of how the rainfall occurrence and intensity change over the course of the year.

We opted to present the application to the particular time series from Exeter, as it is situated in a region where floods pose a real risk to society, and because of the presence of several extreme values (arising from severe storms) which make modelling challenging. The inclusion of splines in every part of the model affords a high degree of flexibility, in the sense that the states can change completely for different times of year and between years. That said, it is possible that there are some climates where the specific model we used to illustrate the framework may not be sufficiently flexible. In this case, the advantage of our approach is that it is fairly trivial to add more wet states, use alternative conditional distributions, combine different conditional distributions, to name just a few potential adaptations. However, as with many statistical endeavours, this comes at the cost of increased complexity, so a balance must be struck to find a model which performs well enough without being impractical.

Finally, in this article we have focussed on modelling the time series from one spatial location. To cater for applications where simulations at more than one location are required, future research will involve combining the innovations presented in this article with methods such as coupled hidden Markov models (Pohle et al., 2018), so that dependence between multiple spatial locations can be allowed for.

References.

- Antonello, M. and R. Roberto (2012). A mixed nonhomogeneous hidden markov model for categorical data, with application to alcohol consumption. *Statistics in Medicine* 31(9), 871–886.
- Aryal, N. R. and O. D. Jones (2017). Fitting the bartlett-lewis rainfall model using approximate bayesian computation. *Proceedings of the 22nd International Congress on Modelling and Simulation*.
- Brooks, S. P. and A. Gelman (1998). General methods for monitoring convergence of iterative simulations. *Journal of Computational and Graphical Statistics* 7(4), 434–455.
- Bruno, B., B. Antonella, and C. Q. Antonio (2008). Using a hidden markov model to analyse extreme rainfall events in centraleast sardinia. *Environmetrics* 19(7), 702–713.
- Chandler, R., V. Isham, P. Northrop, H. Wheeler, C. Onof, and N. Leith (2014). *Uncertainty in Rainfall Inputs*, Chapter Chapter 7, pp. 101–152.
- de Valpine, P., D. Turek, C. J. Paciorek, C. Anderson-Bergman, D. T. Lang, and R. Bodik (2017). Programming with models: Writing statistical algorithms for general model structures with nimble. *Journal of Computational and Graphical Statistics* 26(2), 403–413.
- Dewar, M., C. Wiggins, and F. D. Wood (2012). Inference in hidden markov models with explicit state duration distributions. *IEEE Signal Processing Letters* 19, 235–238.
- Economou, T., T. C. Bailey, and Z. Kapelan (2014, Sep). Mcmc implementation for

- bayesian hidden semi-markov models with illustrative applications. Statistics and Computing 24(5), 739–752.
- Environment Agency (2016). The costs and impacts of the winter 2013 to 2014 floods: Summary.
- Environment Agency (2018). The costs of the winter 2015 to 2016 floods: Summary.
- Furrer, E. M. and R. W. Katz (2008). Improving the simulation of extreme precipitation events by stochastic weather generators. Water Resources Research 44(12), n/a–n/a. W12439.
- Gelman, A., J. Carlin, H. Stern, D. Dunson, A. Vehtari, and D. Rubin (2014, November). Bayesian Data Analysis, Third Edition (Chapman and Hall/CRC Texts in Statistical Science) (Third ed.). London: Chapman and Hall/CRC.
- Kim, Y. and G. Lee (2017, Aug). Stochastic precipitation generator with hidden state covariates. Asia-Pacific Journal of Atmospheric Sciences 53(3), 353–359.
- Kleiber, W., R. W. Katz, and B. Rajagopalan (2012). Daily spatiotemporal precipitation simulation using latent and transformed gaussian processes. Water Resources Research 48(1), n/a–n/a. W01523.
- Li, C., V. P. Singh, and A. K. Mishra (2012). Simulation of the entire range of daily precipitation using a hybrid probability distribution. Water Resources Research 48(3). W03521.
- Meligkotsidou, L. and P. Dellaportas (2011, Jul). Forecasting with non-homogeneous hidden markov models. Statistics and Computing 21(3), 439–449.
- Pohle, J., R. King, M. van der Schaar, and R. Langrock (2018). Coupled markov-switching regression: inference and a case study using electronic health record data. Proceedings of the 33rd International Workshop on Statistical Modelling 1, 242–246.
- R Core Team (2019). R: A Language and Environment for Statistical Computing. Vienna, Austria: R Foundation for Statistical Computing.
- Rayner, D., C. Achberger, and D. Chen (2016). A multi-state weather generator for daily precipitation for the torne river basin, northern sweden/western finland. Advances in Climate Change Research 7(1), 70 – 81.
- Rodriguez-Iturbe, I., D. R. Cox, and V. Isham (1987). Some models for rainfall based on stochastic point processes. Proceedings of the Royal Society of London A: Mathematical, Physical and Engineering Sciences 410(1839), 269–288.
- Scott, S. (2002). Bayesian methods for hidden Markov models: recursive computing in the 21st century. Journal of the American Statistical Association 97, 337–351.
- Segond, M.-L., H. S. Wheeler, and C. Onof (2007). The significance of spatial rainfall representation for flood runoff estimation: A numerical evaluation based on the lee catchment, uk. Journal of Hydrology 347(1), 116 – 131.
- Spezia, L. (2006). Bayesian analysis of non-homogeneous hidden markov models. Journal of Statistical Computation and Simulation 76(8), 713–725.
- Wood, S. (2016). Just another gibbs additive modeler: Interfacing jags and mgcv. Journal of Statistical Software, Articles 75(7), 1–15.
- Yang, C., R. E. Chandler, V. S. Isham, and H. S. Wheeler (2005). Spatial-temporal rainfall simulation using generalized linear models. Water Resources Research 41(11).
- Zucchini, W., I. MacDonald, and R. Langrock (2017, July). Hidden Markov Models for Time Series An Introduction Using R, Second Edition (Chapman and Hall/CRC Monographs on Statistics and Applied Probability (Second ed.)). London: Chapman and Hall/CRC.

E-MAIL: ors203@exeter.ac.uk